A New Parallel XY Nanopositioning Platform Design

Zhengyu Qi

Liaoning University, Department of Physics, No. 66, Chongshan Middle Road, Huanggu District, Shenyang City, China

PKMQi2004@163.com

Abstract. With the development of high-performance linear platforms for producing computer hard disk drive read/write heads and medical devices, nanopositioning systems are becoming increasingly important and have great application prospects in fields such as laser mirror positioning and high-resolution spectrometers. The current nanopositioning systems have a restricted single-axis travel range because of their physical design and the integration process involved. By utilizing established flexible mechanisms in the workplace, a novel large-range nanopositioning system was developed through SolidWorks modeling, with its accuracy confirmed via ANSYS simulation. This design aims to enhance the practical use of large-range nanopositioning systems.

Keywords: Planar motion stage, Parallel robots, Precision, Fabrication.

1 Introduction

A nanopositioning system is a mechatronic motion system with nanometer-scale moving mass [1, 2]. It includes bearings, actuators and drivers, sensors and electronic devices, as well as feedback control implemented on microcontrollers. The advantages of nanopositioning systems lie in their precision, stability, speed, and versatility, which make them indispensable tools in many high-tech fields [3-5].

Nanopositioning bearings[6] offer several benefits, including exceptional precision, minimal friction, and an extended lifespan. Due to the limited number of mechanical parts used in their construction, both friction and backlash are kept to a minimum, which aids in achieving greater accuracy. Additionally, these bearings are designed with considerations for wear and dynamic performance. In contrast to conventional spindle-based technologies, voice coil actuators and magnetic linear drivers provide notable advantages. Moreover, magnetic levitation bearings are particularly well-suited for use in vacuum conditions, giving them a significant edge over traditional air bearings. A nanopositioning actuator[7] is a device designed for precise multi-axis positioning and movement at the nanoscale level. Typically, it consists of several nano-displacement stages and rotational platforms that facilitate the nanoscale manipulation of samples or devices in various directions. This type of system finds widespread use not only in mechanical engineering but also plays an essential role in areas such as semiconductor manufacturing, microscopy, laser technology, and automated production systems. Nanopositioning sensors[8] are mainly used for accurate measurement and positioning at the nanoscale level. These devices take advantage of the unique properties of nanomaterials, including their high specific surface area, distinctive optical characteristics, and advantageous diffusion abilities, to achieve precise control and measurement of tiny objects. Feedback control technology[9] plays a crucial role in nanopositioning, especially in improving both accuracy

CONF-CIAP 2025, January 17-23, Eskisehir, Turkey

DOI 10.4108/eai.17-1-2025.2355236

and stability of positioning. By designing appropriate signal acquisition and control hardware circuits, along with choosing effective feedback control methods, it is possible to significantly reduce the effects of environmental disturbances on positioning stability.

Non-contact bearings[10] eliminate the friction problems present in traditional bearings, thereby reducing wear and heat generation, improving system stability and lifespan. Due to the absence of physical contact, non-contact bearings can achieve higher positioning accuracy and reduce errors caused by mechanical wear. To facilitate the motion orientation of the stage, aerostatic bearings and maglev bearings are typically employed [11]. However, one notable disadvantage of flexible bearings is that their movement range is limited, which restricts the overall movement capability of nanopositioning systems equipped with flexible bases. This limitation arises from the inherent design characteristics of flexible bearings, which are engineered to provide a certain degree of compliance and adaptability in response to external forces. While this flexibility can be advantageous in accommodating misalignments or absorbing vibrations, it simultaneously constrains the extent to which these systems can achieve precise positioning. Nanomotors[12, 13] typically generate very small forces, which limits their ability to effectively or rapidly move larger objects. This constraint is due to the nanoscale at which these motors function; their size is measured in nanometers, making them more suitable for manipulating molecules and particles rather than larger items. In practical scenarios like drug delivery systems within biomedical engineering, the capacity of nanomotors to transport therapeutic agents is vital. However, when they encounter larger biological structures or tissues, their efficiency significantly decreases because of inadequate force production. Moreover, environmental factors such as viscosity and friction at micro- and nanoscale levels can further hinder their movement abilities. The dimensions of actuators[14] are typically constrained by the capabilities of manufacturing technologies, making it more challenging to produce smaller versions. This constraint is due to various factors that are intrinsic to the production methods employed for these components. For example, as an actuator's size diminishes, the level of precision needed in its construction increases markedly. To meet the required specifications at a reduced scale, advanced techniques like micro-machining or additive manufacturing often become essential. The sensors used in nanopositioning systems may struggle with their dynamic range, making it difficult to detect both large and small signals at the same time. This challenge stems from the fundamental properties of the sensor technology, which typically establishes a specific detection threshold. Many sensors are optimized for a particular input level range; however, when they encounter signals that differ greatly in size—common in precision measurement scenarios—their data capture capabilities can be hindered. For example, if a nanopositioning system needs to track tiny positional shifts while also monitoring larger environmental disturbances or variations, the significant difference between these signal magnitudes can result in saturation or clipping. In such cases, smaller signals might become lost amid larger ones, leading to potential loss of vital information essential for accurate control and feedback processes. At the nanoscale[15], the noise from both environmental factors and electronic components can significantly influence measurement outcomes. Environmental disturbances may stem from several sources, including thermal variations, electromagnetic interference, and vibrations in surrounding areas. These elements can introduce inconsistencies into the sensitivity of measurements; for instance, even minor temperature fluctuations can change material characteristics or impact molecular interactions. Additionally, the electronic noise produced by sensors plays a vital role in ensuring measurement accuracy. Some of this noise might mask weak signals that are essential for precise readings at the nanoscale. The interplay between various types of noise complicates data interpretation, necessitating advanced signal processing techniques to derive valuable insights from raw data. As researchers aim for

greater precision in nanotechnology fields like drug delivery systems or nanoscale electronics, the issues related to environmental and electronic noise become more pronounced. Thus, it is not only important to comprehend these influences to enhance measurement methods but also essential to develop more robust sensors capable of functioning effectively under diverse conditions while minimizing errors due to external disruptions. At the nanoscale, various factors like thermal fluctuations, electromagnetic interference, and quantum effects can disrupt signal transmission. Such disruptions may result in data loss or inaccuracies in communication systems that depend on precise information transfer. For example, in nanotechnology fields such as molecular electronics or quantum computing, even slight disturbances can greatly affect the integrity of transmitted signals. The actuators and sensors in a nanopositioning system often necessitate specific environmental conditions for optimal functionality, including regulated temperature, humidity, and vibration isolation. These elements are critical since even slight variations can greatly affect the precision and accuracy of the positioning mechanism. For example, changes in temperature may cause materials within the components to expand or contract thermally, potentially leading to misalignment or positioning errors. Additionally, when these components are incorporated into a larger system or application, compatibility issues might emerge due to differing communication protocols or power needs. Each actuator and sensor could function on varying voltage levels or data transmission standards, which may require extra interfaces or converters for smooth integration. Moreover, electromagnetic interference from adjacent equipment could disrupt sensor readings and actuator efficiency if not properly addressed. Beyond these technical hurdles, it is crucial to take into account the overall design architecture of the nanopositioning system. The configuration must not only fit the physical dimensions of each component but also meet their operational requirements within an integrated framework. This involves ensuring adequate shielding against external disturbances as well as providing sufficient space for maintenance access. In summary, tackling these environmental prerequisites and compatibility challenges is essential for maximizing performance in a nanopositioning system while reducing potential disruptions during its operation.

Based on the existing flexible mechanism, a novel parallel motion XY nanopositioning platform is established via modeling and simulation, and the validity of the physical system is verified [16]. The design of the physical system, which includes bearings, actuators, and sensors, enables a broad XY nanoscale positioning capability. The bearing utilizes a parallel kinematic bending mechanism in the XY plane. By preventing geometric over-constraints, it achieves significant geometric decoupling between the two axes of motion. This design allows for actuator isolation that facilitates the use of large-stroke single-axis actuators and supports various endpoint sensing methods with widely used sensors. These features enable the proposed nanoscale positioning system to achieve a movement range of 10mm × 10mm.

2 Flexible Beam

In order to achieve the large range XY nanopositioning system, bilateral simple parallelogram flexures (BSPF) and bilateral compound parallelogram flexures (BCPF) have been widely used. This section will derive the stiffness of the two structures. The structures of simple parallelogram flexures (SPF) and compound parallelogram flexures (CPF) are shown in the Figure 1.

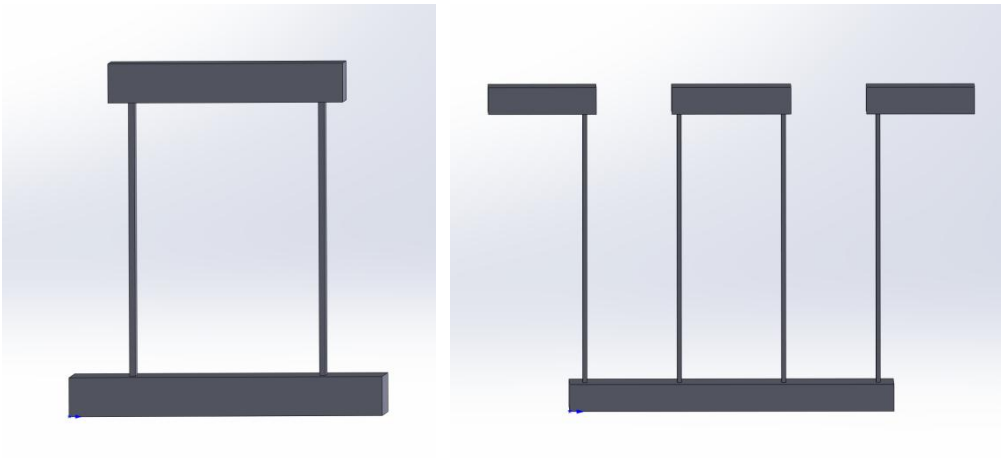

(a) (b)

Fig. 1. Parallelogram flexures. (a) Simple parallelogram flexures (SPF). (b) Compound parallelogram flexures (CPF).

The stiffness of BSPF and BCPF is derived from the CPF model shown in Figure 2 [17].

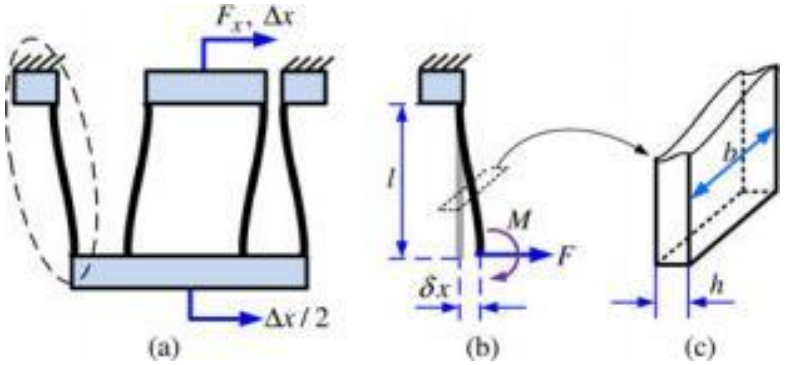

Fig. 2. CPF model. (a) Deformation of a CPF. Dimensions of (b) one flexure and (c) cross section [17].

When an outward force F_x is applied along the X-axis to the CPF, as illustrated in Figure 2(a), it results in a deformation of the CPF's shape. The structure experiences both a force F and a moment M, leading to bending. From this scenario, we can derive the following relationship:

$$0 = \frac{Fl^2}{2EI} - \frac{Ml}{EI} \tag{1}$$

$$\delta_x = \frac{Fl^3}{3EI} - \frac{Ml^2}{2EI} \tag{2}$$

In this equation, δ_x represents the X-axis displacement of a curved body [see Figure 2(b)], E is the Young's modulus of the material, and $I = \frac{bh^3}{12}$ is the moment of inertia about the neutral axis of the cross-section [see Figure 2(c)].

Solving the two equations above allows the generation:

$$F = \frac{2M}{l} \tag{3}$$

$$\delta_x = \frac{Fl^3}{12EI} \tag{4}$$

Given that the lengths of the four curved structures are all equal to l, it follows that $\delta_x = \frac{\Delta x}{2}$, where Δx indicates the displacement on one side of the CPF. Consequently, we can compute the stiffness of the CPF in relation to its output direction:

$$K = \frac{F_x}{\Delta x} = \frac{2F}{2\delta_x} = \frac{Ebh^3}{l^3} \tag{5}$$

The stiffness of the CPF can be obtained by analyzing the stiffness of BSPF and BCPF:

$$K_{\mathrm{BSPF}} = \frac{4Ebh^3}{l^3} \tag{6}$$

$$K_{\mathrm{BCPF}} = \frac{2Ebh^3}{l^3} \tag{7}$$

3 Justification of stiffness of flexible structures

In this section, the stiffness formulas of the BSPF and BCPF from the previous section are validated through SolidWorks modeling and ANSYS simulation. The relationship between structural forces and deformation is illustrated through modeling and simulation. This analysis provides an in-depth examination of multiple factors influencing how structures respond to applied loads. By performing computations, intricate models are created to replicate real-world scenarios. These simulations take into account aspects such as material characteristics, geometric arrangements, boundary conditions, and loading situations.

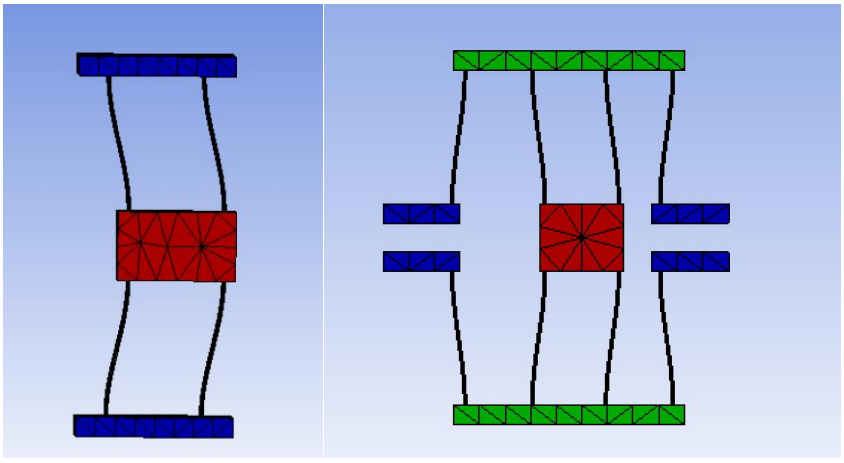

(a) (b)

Fig. 3. Deformation of two structures. (a)Deformation of BSPF. (b) Deformation of BCPF.

3.1 Bilateral simple parallelogram flexures

Assuming l=70mm, b=15mm, h=1.5mm and calculating the stiffness theoretical value of bilateral simple parallelogram flexures through the deduction of the formula, it is 4.1917×10^4 N/m.

Through modeling and simulation, the relationship between structural forces and deformation is shown as follows:

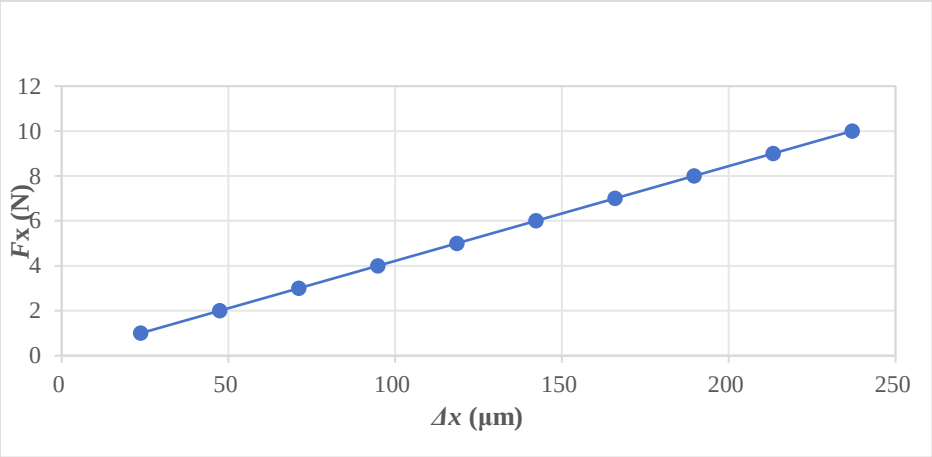

Fig. 4. The relationship between force and deformation of bilateral simple parallelogram flexures.

Through the process of simulation fitting, the actual stiffness value for the bilateral simple parallelogram flexures (BSPF) has been established at 4.2198×10^4 N/m. This measurement is vital for comprehending the mechanical behavior and load-bearing capabilities of such foundations in engineering contexts. The relative error associated with this determination is found to be 0.67%, reflecting a high degree of accuracy in the simulation methodology. The minor discrepancy between the empirical stiffness value obtained and the theoretical estimate derived from established equations indicates that these theoretical models are dependable for predicting performance under comparable conditions. Such validation is crucial as it bolsters confidence in employing these formulas for future design evaluations and analyses.

3.2 Bilateral compound parallelogram flexures

Assuming l=70mm, b=15mm, h=1.5mm and calculating the stiffness theoretical value of bilateral compound parallelogram flexures through the deduction of the formula, it is 2.0958×10^4 N/m.

Through modeling and simulation, the relationship between structural forces and deformation is shown as follows:

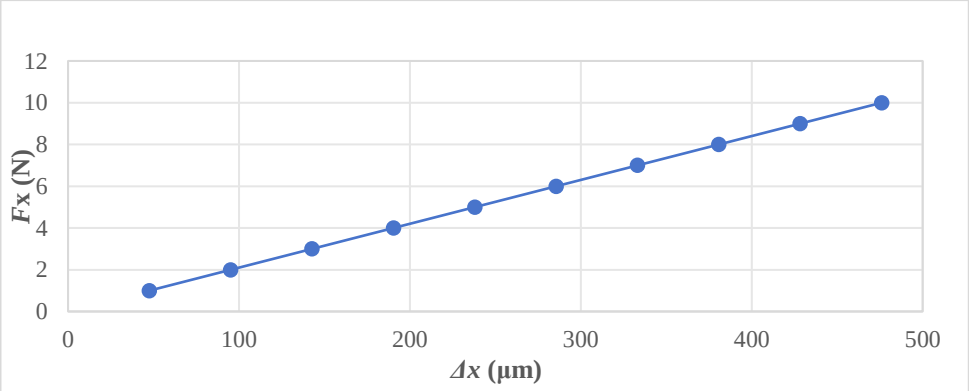

Fig. 5. The relationship between force and deformation of bilateral compound parallelogram flexures.

Through simulation fitting, the actual stiffness of bilateral compound parallelogram flexures (BCPF) has been established at 2.1009×10^4 N/m. This value is crucial for comprehending how the material behaves under different loading scenarios and plays a significant role in its engineering applications. The relative error calculated for this measurement stands at 0.24%, reflecting a high degree of accuracy in the experimental findings. The minor discrepancy between the measured stiffness and theoretical predictions indicates that the formula used for calculations closely reflects real-world behavior. This strong alignment not only confirms the validity of the mathematical model but also enhances confidence in employing such formulas to forecast material properties in future research or applications. Moreover, obtaining accurate measurements like this one is vital for refining design parameters and ensuring reliability in practical uses where BCPF might be applied, including aerospace components, automotive parts, or structural elements that require lightweight yet robust materials. The results from this simulation fitting can act as a benchmark for further investigations aimed at improving composite materials' performance through modifications or alternative formulations.

4 The Establishment and Validation of a New Parallel XY Nanopositioning Platform

In this section, a new parallel XY nanopositioning platform was meticulously designed and constructed using SolidWorks modeling software. The design process was segmented into multiple phases, beginning with the conceptualization of the platform's overall structure to establish essential requirements and specifications for achieving high-precision positioning tasks. Following the conceptual phase, detailed models were created for each individual component to ensure accuracy and functionality.

During the modeling phase, various factors were considered, including size dimensions tailored to specific application needs, material characteristics aimed at enhancing durability and performance under operational conditions, as well as mechanical constraints that could influence assembly and integration with other systems. Each component was modeled independently before being combined into a complete system model to assess compatibility and overall performance. After finalizing the model in SolidWorks, an extensive verification process was necessary to thoroughly evaluate its structural integrity. This assessment employed ANSYS

software for finite element analysis (FEA), which is vital for understanding how different forces interact during operation. FEA offers insights into stress distribution across components under static loads or dynamic impacts among various loading scenarios. The simulation outcomes yielded important data regarding areas prone to excessive stress concentration or potential failure points under standard operating conditions. By pinpointing these critical regions early in the design stage, proactive strategies can be implemented—such as altering geometric designs or opting for alternative materials—to reinforce vulnerable sections without hindering the efficiency of the entire system. This thorough methodology not only confirms the structural soundness of the nanopositioning platform but also establishes a robust foundation for subsequent experimental testing intended for real-world applications.
The modeling and simulation of this structure are shown in Figure 6 and Figure 7.

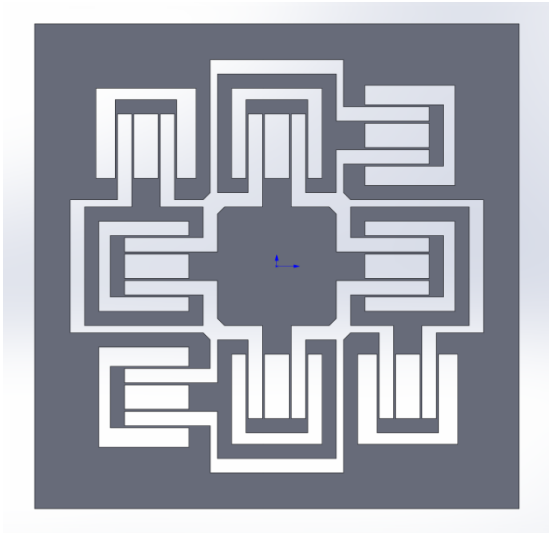

Fig. 6. Modeling of the new parallel XY nanopositioning platform.

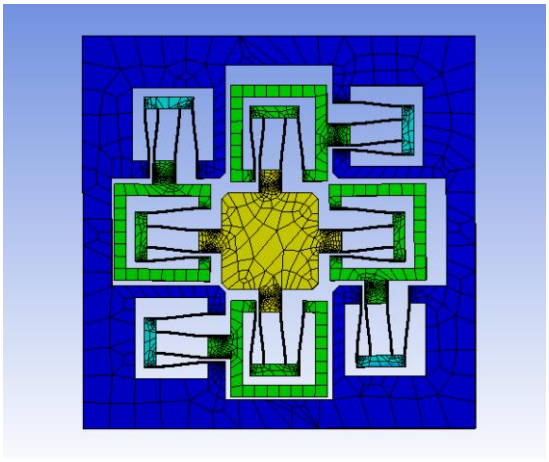

Fig. 7. Simulation of the new parallel XY nanopositioning platform.

The nanopositioning platform is conceptually structured to facilitate the independent functioning of both the X and Y axes. This design ensures that movement along one axis does not influence movement on the other. Specifically, any force exerted in the X direction will solely impact motion along that axis without causing unintended shifts in the Y direction. The principle of decoupling is essential for achieving high-precision positioning tasks, as it enables separate control over each axis. To substantiate this theoretical framework, a detailed derivation was conducted in the article's second section, where extensive analysis of the model's behavior under various conditions was performed. Findings indicate that the single-axis stiffness of this new parallel XY nanopositioning platform is quadruple that of CPF stiffness. A novel K value for single-axis performance has been defined for this innovative parallel XY nanopositioning system, which plays a vital role in understanding how effectively it reacts to forces and displacements applied to each individual axis. The calculation method for this K value integrates empirical data from testing with theoretical insights derived from modeling efforts. Through thorough analysis and inventive design strategies aimed at enhancing axial independence and stiffness properties, a robust foundation has been laid for precise motion control in advanced applications necessitating fine positioning capabilities.

We can obtain the new single-axis K value of the new parallel XY nanopositioning platform as follows:

$$K = \frac{4Ebh^3}{l^3} \tag{8}$$

Set the b to 30mm, h to 1.5mm and l to 45 mm during the modeling process. The material is aluminum, with a Young's modulus of 71 GPa. According to the single-axis stiffness formula derived above, the theoretical value is 3.1556×10^5N/m.

By using simulation technology and graphical analysis, the specific relationship between force and deformation in the X and Y axes was determined after applying pressure to both axes simultaneously. The method includes systematically adjusting the applied force and recording the deformation generated in each direction. These simulations are intended to simulate real-life conditions in order to accurately evaluate the performance of the nanopositioning platform under load. By studying these interactions, we can see how changes in force directly affect the displacement of each axis.

The resulting relationship graph is presented below:

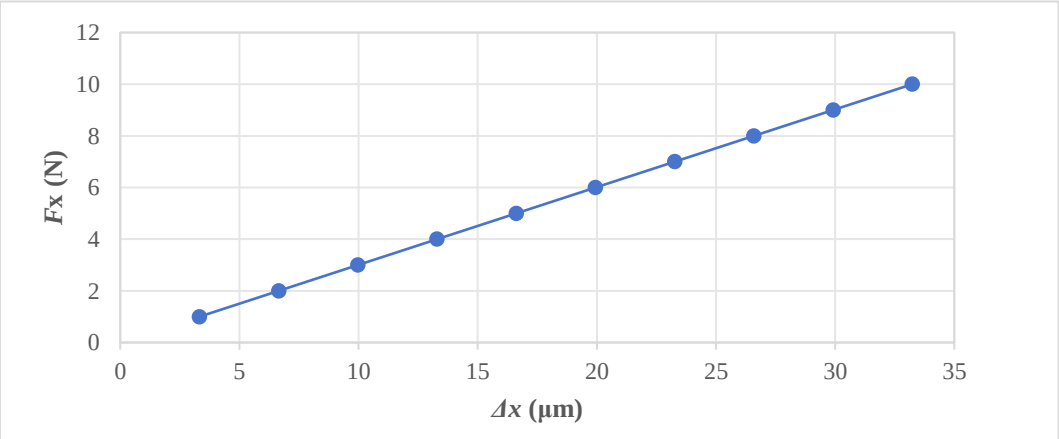

Fig. 8. The correlation between force and deformation along the X-axis.

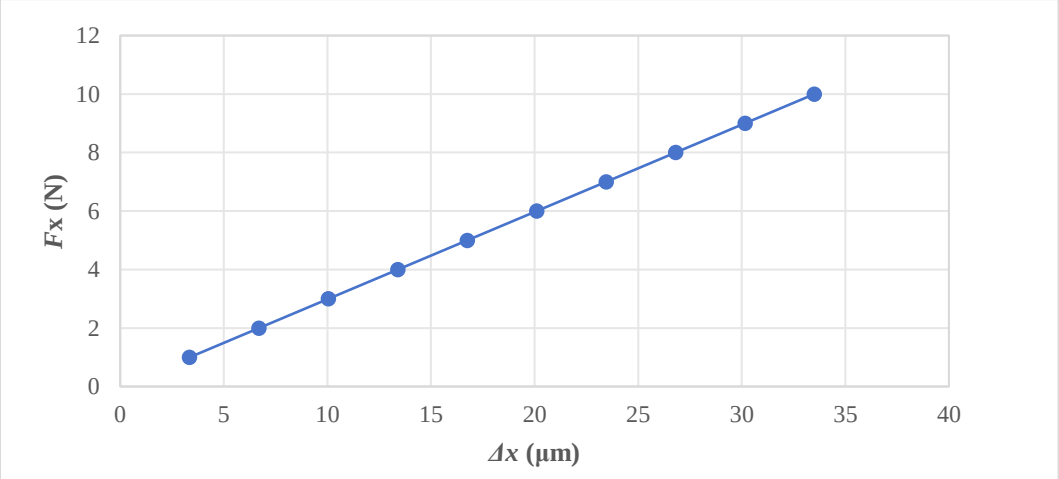

Fig. 9. The correlation between force and deformation along the Y-axis.

The graphical fitting analysis revealed that the stiffness in the X direction measured 3.0086×10^5 N/m, whereas in the Y direction it was recorded at 2.9840×10^5 N/m. This information is vital for comprehending how each axis reacts to applied forces, which is critical for assessing the overall functionality of the nanopositioning platform. The relative error for stiffness in the X direction was -4.66%, indicating a slight deviation from what was theoretically anticipated. In a similar vein, the relative error for stiffness in the Y direction stood at -5.44%. These results suggest that the observed stiffness values align closely with theoretical predictions derived from initial design parameters and modeling efforts. Confirming structural accuracy through experimental data can bolster confidence in both reliability and effectiveness of the nanopositioning system during practical applications. Furthermore, these findings lay a groundwork for future enhancements and optimization of design frameworks aimed at improving axial performance characteristics even further. Grasping how experimental outcomes relate to theoretical expectations will facilitate ongoing advancements in precision engineering across various domains.

5 Conclusion

This study conducted an in-depth analysis of standard flexible structures, leading to the development of stiffness equations for bilateral simple parallelogram flexures (BSPF) and bilateral compound parallelogram flexures (BCPF). The research encompassed both theoretical evaluations and practical modeling and simulation efforts. Detailed geometric representations and structural assessments of BSPF and BCPF were created using SolidWorks. Subsequently, simulations were performed in ANSYS to validate the derived stiffness equations for BSPF and BCPF under different loading scenarios. The findings from these analyses demonstrated that the models accurately represented the anticipated performance metrics. Additionally, this research introduced a novel parallel XY nanopositioning platform, achieving measured X-axis stiffness at 3.0086×10^5 N/m and Y-axis stiffness at 2.9840×10^5 N/m. Notably, these measurements showed minimal deviation from the theoretically predicted values of 3.1556×10^5 N/m, underscoring the reliability of the employed modeling techniques. The implementation of this

nanopositioning system has significantly expanded its motion range compared to previous designs. This enhancement is projected to improve operational efficiency across various applications while bolstering capabilities in fields requiring precise positioning systems. Furthermore, this framework establishes a vital groundwork for advancing large-range nanopositioning technologies and offers valuable insights into effective design strategies suitable for diverse situations. As a result, it is anticipated that real-world applications will reap benefits from these innovations by enabling higher precision complex tasks over broader ranges.

References

[1] X Ding, J S Dai. Compliance Analysis of Mechanisms with Spatial Continuous Compliance in the Context of Screw Theory and Lie Groups[J]. Proceedings of the Institution of Mechanical Engineers, Part C: Journal of Mechanical Engineering Science, 2010, 224 (11): 2493-2504.

[2] Choi, J., Hong, S., Lee, W., Kang, S., Kim, M.. A Robot Joint With Variable Stiffness Using Leaf Springs[J]. IEEE Transactions on Robotics: A publication of the IEEE Robotics and Automation Society, 2011, 27 (2): 229-238.

[3] Santosh Devasia, Evangelos Eleftheriou, S. O. Reza Moheimani. A Survey of Control Issues in Nanopositioning.[J]. IEEE Trans. Contr. Sys. Techn., 2007, 15 (5): 802-823.

[4] Byoung Hun Kang, John T. Wen, Nicholas G. Dagalakis, Jason Gorman. Analysis and Design of Parallel Mechanisms with Flexure Joints.[J]. IEEE Trans. Robotics, 2005, 21 (6): 1179-1185.

[5] Jonathan B. Hopkins, Martin L. Culpepper. Synthesis of Multi-degree of Freedom, Parallel Flexure System Concepts via Freedom and Constraint Topology (FACT) - Part I: Principles[J]. Precision Engineering, 2010, 34 (2): 259-270.

[6] Cui Mengjia, Shang Erwei, Jiang Shouqian, Liu Yu, Zhang Zhen. Design, Fabrication and Implementation of a High-performance Compliant Nanopositioner via 3D Printing with Continuous Fiber-reinforced Composite[J]. Journal of Micromechanics and Microengineering, 2021, 31 (12).

[7] Vickers Nicholas A, Andersson Sean B. Synthetic Stochastic Motion Platform for Testing Single Particle Tracking Microscopes.[J]. IEEE transactions on control systems technology : a publication of the IEEE Control Systems Society, 2022, 30 (6): 2726-2733.

[8] Simon Brecht G, Kurdi Samer, Carmiggelt Joris J, Borst Michael, Katan Allard J, van der Sar Toeno. Filtering and Imaging of Frequency-Degenerate Spin Waves Using Nanopositioning of a Single-Spin Sensor.[J]. Nano letters, 2022, 22 (22).

[9] Nava Rezvani, Ali KeymasiKhalaji. Adaptive RBFNN ‐ based Predictive Control for the Nanopositioning of an Electrostatic MEMS Actuator[J]. IET Control Theory & Applications, 2023, 18 (5): 551-565.

[10] Nan Wang, Zhe Yuan, Peng Wang. Dynamic Electromagnetic Force Variation Mechanism and Energy Loss of a Non-contact Loading Device for a Water-lubricated Bearing[J]. Journal of Mechanical Science and Technology, 2021, 35 (6): 1-12.

[11] W Dong, J Tang, Y ElDeeb. Design of a Linear-motion Dual-stage Actuation System for Precision Control[J]. Smart Materials and Structures, 2009, 18 (9): 095035 (11pp)

[12] Sharmila N Shirodkar, Tonghui Su, Nitant Gupta, Evgeni S Penev, Boris I Yakobson. Mechanical Efficiency of Photochromic Nanomotors, From First Principles.[J]. Small (Weinheim an der Bergstrasse, Germany), 2024, e2400305.

[13] Mohammadbagher Mohammadnezhad, Salah Raza Saeed, Sarkew Salah Abdulkareem, Abdollah Hassanzadeh. Light-driven Nanomotors with Reciprocating Motion and High Controllability based on Interference Techniques.[J]. Nanoscale advances, 2024, 6 (4): 1122-1126.

[14] Karrar A. Hassan, Furat I. Hussein, Wisam S. Hacham. Design and Fabrication of an Electromechanical Tester to Perform Two-dimensional Tensile Testing for Flexible Materials[J]. American Academic Scientific Research Journal for Engineering, Technology, and Sciences, 2022, 90 (1): 41-51.

[15] Paloma L Ocola, Ivana Dimitrova, Brandon Grinkemeyer, Elmer Guardado Sanchez, Tamara Đorđević, Polnop Samutpraphoot, Vladan Vuletić, Mikhail D Lukin. Control and Entanglement of Individual Rydberg Atoms near a Nanoscale Device.[J]. Physical review letters, 2024, 132 (11): 113601-113601.

[16] Shorya Awtar, Gaurav Parmar. Design of a Large Range XY Nanopositioning System[J]. Journal of Mechanisms and Robotics: Transactions of the ASME, 2013, 5 (2): 021008-1-021008-10.

[17] Qingsong Xu. New Flexure Parallel-Kinematic Micropositioning System With Large Workspace[J]. IEEE Transactions on Robotics: A publication of the IEEE Robotics and Automation Society, 2012, 28 (2): 478-491.